of these regions in AD (*3–8*). This also implies that with the MRI-guided method we have actually compensated the CBF measurements for atrophy. The partial volume effects of SPECT still make it impossible to clearly rule out atrophy as the cause of the CBF reduction. However, in the clinical context, it may be more interesting if we find that better separation is achieved between AD and control subjects by combining volume and CBF data than by either volume or CBF alone.

CONCLUSION

This study shows that reliable measurements of medial temporal lobe blood flow can be performed by MRI-guided SPECT measurements. The error of interactive alignment was less than one SPECT pixel size. The CV of the medial temporal-to-cerebellar CBF ratio found in this study was only 3.2%. In patients with AD, it was possible to detect clear reductions in blood flow in the medial temporal lobes with high reliability using MRI-defined cerebellar reference and also using healthy whole-brain reference regions created by three-dimensional region growing. Also, the volumes of the medial temporal lobes were smaller in the AD group. The best separation between the groups was found when combining medial temporal volume and blood flow data into a composite z-score. Larger clinical studies are needed to evaluate if the combination of MRI and SPECT measurements of medial temporal lobe changes can improve the early diagnosis of AD.

ACKNOWLEDGMENTS

This study was supported by the Municipal Pensions Institute.

REFERENCES

1. Braak H, Braak H. Neuropathological staging of Alzheimer-related changes. *Acta Neuropathol* 1991;82:239–256.
2. Almkvist O, Bäckman L. Detection and staging of early clinical dementia. *Acta Neurol Scand* 1993;88:10–15.
3. Seab JP, Jagust WJ, Wong ST, Roos MS, Reed BR, Budinger TF. Quantitative NMR measurements of hippocampal atrophy in Alzheimer's disease. *Magn Reson Med* 1988;8(2):200–208.
4. Jack CJ, Petersen RC, O'Brien PC, Tangalos EG. MR-based hippocampal volumetry in the diagnosis of Alzheimer's disease. *Neurology* 1992;42:183–188.
5. Scheltens P, Leys D, Barkhof F, et al. Atrophy of medial temporal lobes on MRI in "probable" Alzheimer's disease and normal aging: diagnostic value and neuropsychological correlates. *J Neurol Neurosurg Psychiatry* 1992;55:967–972.
6. Wahlund LO, Andersson-Lundman G, Basun H, et al. Cognitive functions and brain structures: a quantitative study of CSF volumes on Alzheimer patients and healthy control subjects. *Magn Reson Imaging* 1993;11:169–174.
7. de Leon MJ, Golomb J, George AE, et al. The radiologic prediction of Alzheimer's disease: the atrophic hippocampal formation. *AJNR* 1993;14:897–906.
8. Killiany RJ, Moss MB, Albert MS, Sandor T, Tieman J, Jolesz F. Temporal lobe regions on magnetic resonance imaging identify patients with early Alzheimer's disease. *Arch Neurol* 1993;50:949–954.
9. Slomka PJ, Hurwitz G, Stephenson JA, Cradduck TD. Automated alignment and sizing of myocardial stress and rest scans to three-dimensional normal templates using an image registration algorithm. *J Nucl Med* 1995;36:1115–1122.
10. Slomka PJ, Hurwitz GA, St Clement G, Stephenson J. Three-dimensional demarcation of perfusion zones corresponding to specific coronary arteries: application for automated interpretation of myocardial SPECT. *J Nucl Med* 1995;36:2120–2126.
11. Lassen NA, Andersen AR, Friberg L, Paulson OB. The retention of ^{99m}Tc-d,l-HM-PAO in the human brain after intracarotid bolus injection: a kinetic analysis. *J Cereb Blood Flow Metab* 1988;8:S13–S22.
12. Pietrzyk U, Herholz K, Fink G, et al. An interactive technique for three-dimensional image registration: validation for PET, SPECT, MRI and CT brain studies. *J Nucl Med* 1994;35:2011–2018.
13. Harris GJ, Pearlson GD. MRI-guided region of interest placement on emission computed tomograms. *Psych Res* 1993;50:57–63.
14. Syed GMS, Eagger S, Toone BK, Levy R, Barret JJ. Quantification of regional cerebral blood flow (rCBF) using ^{99}Tc^{m}-HMPAO and SPECT: choice of the reference region. *Nucl Med Commun* 1992;13:811–816.

Comparative Quantitation of Cerebral Blood Volume: SPECT Versus PET

Andrei Vlasenko, Marie-Christine Petit-Taboué, Gerard Bouvard, Rémy Morello and Jean-Michel Derlon

CYCERON, Biomedical Cyclotron Centre CEA/DRM, Centre F. Baclesse and Departments of Nuclear Medicine, Neurosurgery and Computer Science, University Hospital, University of Caen, Caen, France, and Institute of Neurology, Moscow, Russia

Quantification of cerebral blood volume (CBV) measured by SPECT has been used for evaluation of cerebral hemodynamics in patients with cerebrovascular diseases. The accuracy of such quantification, however, has not been validated with PET. **Methods:** CBV was assessed using SPECT and in vitro ^{99m}Tc-labeled red blood cells and PET with the ^{15}O steady-state inhalation method and C^{15}O. In 23 patients with carotid artery disease, we measured hemispheric (including cortical and subcortical areas) CBV, and in 11 patients, we measured regional CBV in small cortical regions. We further evaluated the interhemispheric and inter-regional asymmetry of CBV with both methods. **Results:** Quantitative values of both hemispheric and regional CBV measured by SPECT were significantly correlated with those measured by PET in the same patients. There was a significant correlation between the side-to-side asymmetry of CBV for both methods. **Conclusion:** This study demonstrates usefulness and the accuracy of SPECT for quantitative CBV assessment in comparison with the less widely available PET procedures.

Key Words: cerebral blood volume; PET; SPECT

J Nucl Med 1997; 38:919–924

Received Mar. 25, 1996; revision accepted Oct. 30, 1996.

For correspondence or reprints contact: Marie-Christine Petit-Taboué, MD, CYCERON, Boulevard Henri Becquerel, B.P. 5229, 147074, Caen CEDEX, France.

Occlusive carotid artery disease with insufficient collateral supply results in a dilatation of the peripheral vessels that compensates for the decrease in cerebral perfusion pressure (*1*). In regions where compensatory dilatation has already occurred, vasodilatory capacity is diminished and such regions are assumed to be more susceptible to an ischemic stroke of both a hemodynamic and embolic origin. Therefore, evaluation of the vasodilatory capacity could contribute to management of patients with internal carotid artery (ICA) disease.

Measurements of cerebral blood flow (CBF) with or without inhalation of carbon dioxide (*2,3*) or injection of acetazolamide (*4,5*) may be useful for an assessment of this vasodilatory capacity. Cerebral blood volume (CBV) is also a major factor in the regulation of cerebral hemodynamics (*6*). Augmentation of CBV is associated with the dilatation of pial vessels, as the consequence of decreased perfusion pressure, and may itself reflect a diminished vasodilatory capacity. Moreover, combined measurements of CBF and CBV allow one to evaluate the CBF/CBV ratio. This ratio has been reported previously as being a reliable index of the local cerebral perfusion pressure (*6–8*). Thus, the assessment of CBV has a particular significance in cerebrovascular diseases.

Several methods for measuring CBV have been proposed (*9*), with PET being the most reliable method. However, PET is

TABLE 1
Clinical, CT and Angiographical Characteristics of Patients

Patient no.	Clinical manifestations	CT data	Angiographic data
1	TIA	+	Unilateral stenosis
2	TIA	+	Unilateral occlusion
3	TIA	−	Unilateral occlusion
4	No symptoms	+	Unilateral stenosis
5	Stroke	−	Unilateral occlusion
6	Stroke	+	Bilateral stenoses
7	Stroke	No CT data	Bilateral stenoses
8	Stroke	+	Unilateral occlusion
9	Stroke	+	Occlusion plus stenosis
10	No symptoms	−	Unilateral occlusion
11	TIA	−	Occlusion plus stenosis
12	TIA	+	Unilateral stenosis
13	TIA	+	Unilateral stenosis
14	Stroke	+	Unilateral stenosis
15	TIA	−	Unilateral stenosis
16	TIA	+	Unilateral stenosis
17	Stroke	+	Unilateral stenosis
18	Stroke	+	Unilateral occlusion
19	Stroke	+	Bilateral occlusion
20	TIA	−	Unilateral stenosis
21	TIA	−	Bilateral stenoses
22	No symptoms	−	Bilateral stenoses
23	TIA	−	Unilateral stenosis

+ = unilateral brain infarction; − = no CT lesion.

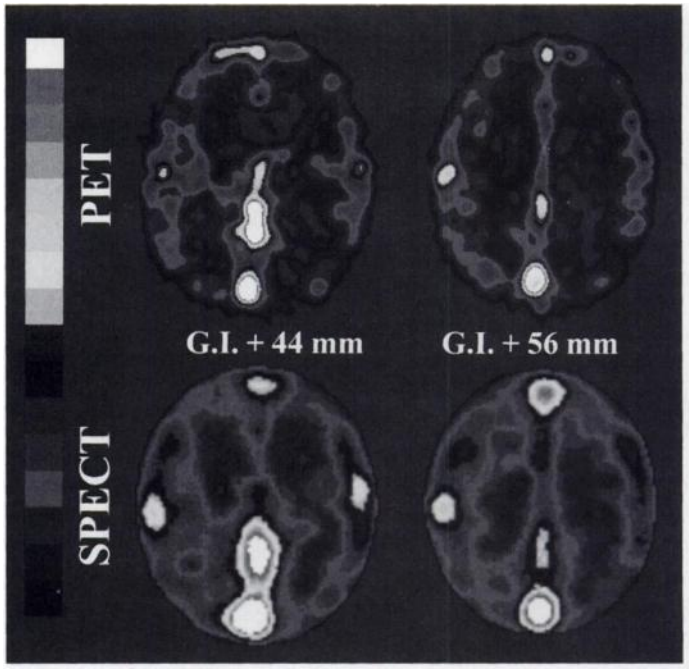

FIGURE 1. CBV images reconstructed in two selected planes (GI + 44 mm and GI + 56 mm) using PET and SPECT.

expensive and is not readily available in many institutions. As such, its use for routine measurement of CBV is significantly limited.

SPECT is another method that has been suggested for the assessment of CBV. Only semiquantitative or quantitative CBV measurements using SPECT have been reported to date (*10–17*), and the ability of SPECT to quantify CBV accurately has been questioned (*7,18*). Moreover, there are no studies in which CBV values (quantified using SPECT) have been compared with those measured by PET in the same subjects.

The aim of the present investigation was to quantify CBV in patients with ICA disease and to compare hemispheric and regional CBV values as well as the side-to-side asymmetry of CBV measured by SPECT with those of the same patients measured by PET.

MATERIALS AND METHODS

SPECT and PET measurements were performed in 23 patients (18 men and 5 women; mean age, 63.3 ± 9.2 yr) with ICA disease (Table 1). There were 11 patients with transient ischemic attacks (TIAs), 9 patients with completed stroke and 3 patients without any neurological symptoms. In 22 patients, a CT scan was performed (CGR ND-12000, Compagnie Générale de Radiologie, Buc, France), which revealed a normal brain (n = 9) or a unilateral hypodensity of ischemic origin (n = 13). All patients underwent an angiography of at least both ICAs, showing unilateral (n = 6) or bilateral (n = 1) occlusion, unilateral (n = 10) or a bilateral (n = 4) hemodynamically significant (>75%) stenosis or a combination of occlusion with contralateral stenosis (n = 2).

All patients gave their informed consent to the dual isotopic assessment of brain hemodynamics. These studies have been approved by the ethical committee at the University Hospital of Caen (France).

PET Study

Tomographic images of CBV were obtained using ^{15}O steady-state inhalation method with $C^{15}O$ (*19*) and a 7-slice LETI TTV03 time-of-flight camera (intrinsic resolution, 5.5 × 5.5 × 9 mm, x,y,z; Laboratoire d'Electronique et de Techniques Informatiques, Grenoble, France). The $C^{15}O$ gas was produced and delivered by a baby cyclotron (CYPRIS 325 model, Compagnie Générale de Radiologie, Buc, France).

The patient was positioned comfortably, and a Laitinen stereotactic frame (Issal Surgical Instruments, Stockholm, Sweden) was fitted to the head and then fixed onto the PET couch. We used a method described by Fox et al. (*20*) for positioning based on the glabela–inion line (GI) determined on a lateral skull x-ray. This line is parallel to the axis between the anterior and the posterior commissures and allows one to define the PET planes in according to a brain stereotaxic atlas (*21*). Using external and medial laser beams, the PET camera was tilted according to references from the Laitinen frame in order to obtain seven planes parallel to the GI line: −4, + 8, + 20, + 32, + 44, + 56 and + 68 mm.

Before the study, a thin catheter was inserted into the radial artery under local anesthesia with lidocaine. Duplicate samples of blood were drawn via this arterial catheter every 5 min. Blood and plasma samples were counted to determine the radioactivity, which was corrected for the physical decay of ^{15}O. The $PaCO_2$, PaO_2, pH, hematocrit, arterial hemoglobin and carboxyhemoglobin were also measured frequently.

A transmission scan was performed using an external source of ^{68}Ge in order to correct emission scans for photon attenuation.

Oxygen-15-carbon monoxide was delivered at trace doses in air and was inhaled by the patient via an oxygen face mask. Gas flow and radioactivity concentrations were continuously monitored to assume a good equilibrium. The rate of radioactivity delivery for $C^{15}O$ was 407 MBq/min. About 7 min were necessary to reach the steady state. Acquisition of data was then commenced over 10 min.

The PET images were then transformed pixel by pixel into quantitative CBV (ml/100 ml) images using ^{15}O blood data according to previously validated equations (*22*).

For our purposes we selected two planes: GI + 44 mm and GI

TABLE 2
Mean Hemispheric CBV (±s.d.) and Coefficients of Correlation (r) Between PET and SPECT in 23 Patients with ICA disease

	Right hemisphere			Left hemisphere		
	Plane 1	Plane 2	Mean*	Plane 1	Plane 2	Mean*
PET	3.06 ± 0.52	2.82 ± 0.53	2.92 ± 0.52	2.96 ± 0.55	2.69 ± 0.49	2.83 ± 0.45
SPECT	3.03 ± 0.51	2.82 ± 0.53	2.94 ± 0.53	2.97 ± 0.48	2.7 ± 0.37	2.82 ± 0.53
r	0.92†	0.87†	0.9†	0.87†	0.73†	0.82†

*Mean values for both planes.
†$p < 0.01$.

+ 56 mm (Fig. 1). Analysis of the PET data was performed according to a standardized region-of-interest (ROI) procedure independent of PET images (*23*), as follows. First, CT scan planes according to the seven PET planes were obtained, perfect matching of the two imaging modalities being ensured at the time of scanning with reference to the GI line. Accurate contour superimposition of matched PET and CT datasets within the display matrix were obtained thanks to a dedicated user-interactive software. Delineation of ROIs was then performed on CT scan cuts according to the Talairach's stereotaxic atlas (*21*) with respect to the GI line (which has known relationships with the anterior commissure-posterior commissure reference point). First, large hemispheric ROIs were defined on CT scan of both selected planes, which corresponds on PET images approximately to an isocontour set at 50% of the maximal pixel radioactivity of each plane. Thereafter, it was copied onto the opposite side through the use of mirror image function. Second, circular ROIs (diameter, 14 mm) were placed along the cortical ribbon and in the subcortical areas, according to a standardized procedure described in detail elsewhere (*23*). At the levels of GI + 44 mm and GI + 56 mm, 18 and 15 ROIs were defined, respectively. Special care was taken to avoid the regions over the venous sinuses.

The interhemispheric or inter-regional ratio was expressed by the index of asymmetry (IA): IA = 2 × (right CBV − left CBV)/(right CBV + left CBV).

SPECT Study

SPECT measurements were performed 24 hr after the PET examination. Technetium-99m-labeled red blood cells (740 MBq) (in vitro technique, TCK 11, CIS Bio International) were injected intravenously. SPECT scanning of the head began 20 min after injection.

Before the acquisition, the GI line, identified during the PET study, was marked with two point sources. The patient's head was fixed with the GI line being perpendicular to the axis of rotation.

Studies were undertaken using a rotating digital gamma camera (Elscint Apex 409 ECT) equipped with a high-resolution, low-energy collimator. The radius for the rotation of the camera was set at 23 cm, and projection data on 360° were continuously recorded during 25 min through a 64 × 64 matrix in 90 equal angular samples. After scanning, two blood samples were withdrawn from the antecubital vein of the arm opposite the injection site.

Acquisition was made using the dual-energy window technique (*24*). Two blood volume images (14 mm) were reconstructed parallel to the GI line (GI + 44 mm and GI + 56 mm) by the filtered backprojection method (Fig. 1). Hanning filters with cut-off frequencies of 0.73 cycles · cm^{-1} for the first window (photopeak events, 126–154 keV) and approximately 0.36 cycles · cm^{-1} for the second window (scattered events, 92–124 keV) were used. To reduce the scatter effect, a fraction of 0.5 of the Compton reconstructed images was subtracted from the photopeak reconstructed images (*24*). The method described by Chang (*25*) was used for the attenuation correction assuming an ellipse for the patient head outline and a value of 0.15 cm^{-1} for the attenuation correction. To minimize head contour errors, two different ellipses were defined for the two slices and their major axes were obtained from the PET data at the same level.

Calibration of the SPECT system was performed using a skull phantom filled with water and different concentrations of ^{99m}Tc. Emission scans of the phantom were obtained using the same parameters of acquisition and reconstruction as for the patients. A regression equation was obtained for these data to compare the scan data with the activity measured directly from the phantom. This regression equation was used to determine the concentration of ^{99m}Tc-labeled red blood cells in subject's scan (*11,26*).

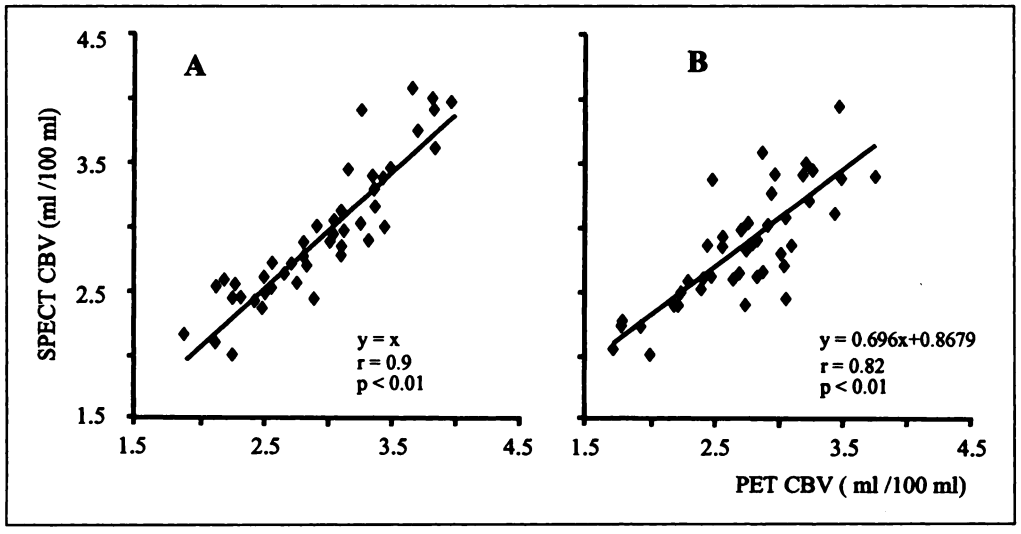

FIGURE 2. Correlation between hemispheric CBV values measured by PET and SPECT in 23 patients with ICA disease for right (A) and left (B) hemispheres.

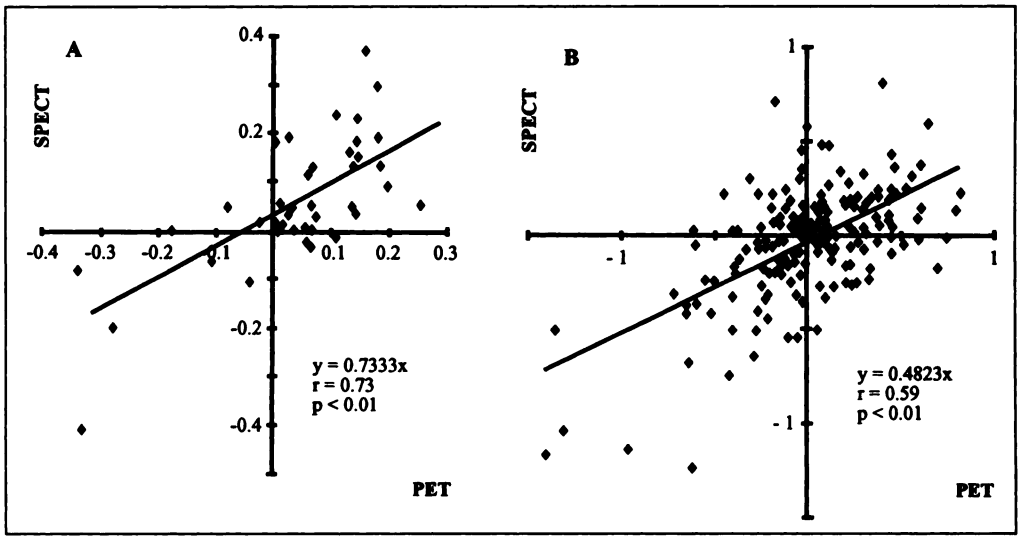

FIGURE 3. Correlation between IA of hemispheric (A) and regional (B) CBV measured by PET and SPECT in 23 patients with ICA disease.

The two SPECT planes were than transformed pixel by pixel into quantitative CBV (ml/100 ml) images according to the equation:

$$CBV = \frac{C_{br}}{0.85 \cdot Ht \cdot C_{rbc} + (1 - 0.85 \cdot Ht) \cdot C_{pl}} \times 100,$$

where C_{br} is the activity per milliliter of brain determined by scan (using regression equation), Ht is the peripheral large-vessel hematocrit (measured directly in the blood samples), 0.85 is the cerebral hematocrit correction (ratio of the cerebral small-vessel hematocrit to the large-vessel hematocrit), C_{rbc} and C_{pl} are the activities per milliliter of red blood cells and plasma from blood samples, respectively, and 100 converts local CBV values to milliliter per 100 milliliters of the brain.

Identical hemispheric and regional ROIs as those used in the PET studies were determined on both selected planes to calculate hemispheric and regional CBV values.

The interhemispheric or inter-regional ratio was expressed by the IA, which was calculated as in the PET study.

Statistical Analysis

Statistical significance was assessed using correlation analysis and paired or unpaired Student's t-test. For every line regression, the slope and the constant values have been tested at 1 and 0, respectively.

RESULTS

Hemispheric CBV

In all 23 patients, we compared hemispheric CBV measured by PET and SPECT and calculated the mean values ± s.d. of CBV for both planes and for both hemispheres (Table 2). PET values of CBV for the right hemisphere were greater than for the left hemisphere, but this difference was statistically significant only for mean values summed for both planes ($p < 0.01$). SPECT values of CBV for the right hemisphere were also somewhat greater than for the left hemisphere, but this difference was not statistically significant. There was a significant correlation between PET and SPECT values for both planes and hemispheres. Coefficients of correlation varied from 0.73 to 0.92 ($p < 0.01$). The results of a correlation analysis between PET and SPECT values of CBV for both planes are illustrated in Figure 2. There was a significant correlation for both right and left hemispheres. Coefficient of correlation was 0.9 for the right hemisphere. The expected regression line was $y = x$. The slope and the constant were not significantly different from 1 and 0, respectively. The coefficient of correlation was 0.82 for the left one ($p < 0.01$). The expected regression line was $y = 0.696x + 0.8679$. The slope and the constant were significantly different from 1 ($p < 0.001$) and 0 ($p < 0.001$), respectively.

IA of Hemispheric CBV

We also looked for a correlation between IA of hemispheric CBV calculated for both planes according to the above described equation (Fig. 3A). Individual values of IA had the sign "–" in those cases when CBV for the left hemisphere was greater than for the right one. This correlation was found to be significant ($r = 0.73$, $p < 0.01$). The expected regression line was $y = 0.7333x$. The slope was significantly different from 1 ($p < 0.02$). The constant did not differ significantly from 0.

Regional CBV

Because we found a significant correlation between both methods for large hemispheric ROIs, we have quantified CBV for the smaller regional ROIs. We analyzed 218 ROIs in 11 patients. Regional values of CBV measured by PET and SPECT, and the results of a correlation analysis are presented in Table 3. There was no significant difference between PET and SPECT values of CBV for both hemispheres. However, the coefficients of correlation varied from 0.49 to 0.78 ($p < 0.01$).

Statistical Analysis

The results of a correlation analysis of regional CBV measured by PET and SPECT are presented in Figure 4. Figure 4A illustrates the correlation between CBV values for right hemisphere. The coefficient of correlation was 0.77 ($p < 0.01$). The expected regression line is $y = 0.653x + 0.919$. The slope and the constant differed significantly from 1 ($p < 10^{-17}$) and 0 ($p < 10^{-10}$), respectively. The correlation between CBV values for left hemisphere (Fig. 4B) was less than for right hemisphere but also significant ($r = 0.62$, $p < 0.01$). The expected regression line was $y = 0.538x + 1.385$. The slope and the constant differed significantly from ($p < 10^{-19}$) and 0 ($p < 10^{-15}$), respectively.

IA of Regional CBV

Finally, we compared the IA of regional CBV measured by PET and SPECT (Fig. 3B). As described above for the IA of hemispheric CBV, individual regional values had the sign "–" when CBV for left hemisphere was greater than for the left one. The correlation between IA of regional CBV was also found to be significant ($r = 0.59$, $p < 0.01$). The expected regression line

TABLE 3
Mean Regional CBV (±s.d.) and Coefficients of Correlation (r) Between PET and SPECT in 11 Patients with ICA Disease

	Right hemisphere			Left hemisphere		
	Plane 1	Plane 2	Mean*	Plane 1	Plane 2	Mean*
PET	3.42 ± 1.2	3.19 ± 1.13	3.32 ± 1.18	3.33 ± 1.1	3.23 ± 1.06	3.29 ± 1.08
SPECT	3.17 ± 1.0	2.98 ± 0.99	3.09 ± 1.0	3.25 ± 0.99	3.03 ± 0.85	3.15 ± 0.93
r	0.76†	0.7†	0.77†	0.78†	0.49†	0.62†

*Mean values for both planes.
†$p < 0.01$.

was y = 0.482x. The slope was significantly different from 1 ($p < 10^{-23}$). The constant did not differ significantly from 0.

DISCUSSION

Quantitative tomographic measurements of hemispheric and regional CBV in humans using SPECT and ^{99m}Tc-labeled red blood cells have been studied by several authors (*11,14,26,27*). Regional CBV has been determined using PET with ^{11}CO-labeled red blood cells (*28*) or the ^{15}O steady-state inhalation method (*19,23,29*). In the literature, regional CBV values measured by PET and SPECT in normal healthy volunteers ranged from 3.2 ± 0.3 ml/100 ml (*14*) to 5.1 ± 0.41 ml/100 ml. Thus, the feasibility of quantitative measurements of hemispheric and regional CBV has been documented, but no study to date has been performed to compare regional and hemispheric CBV measured by PET and SPECT in the same patients and the same planes.

Through the use of ^{99m}Tc-labeled red blood cells, we measured hemispheric (large regions including cortical as well as subcortical areas) and regional (circular cortical ROIs) CBV with SPECT and PET. Our data indicate that quantitative values of both hemispheric and regional CBV measured by SPECT are significantly correlated with those measured by PET in patients with ICA disease.

There was a significant correlation between the side-to-side asymmetry of CBV measured either with SPECT and PET. The correlation was better for large hemispheric ROIs than for the regional ones.

For SPECT, the in vitro labeling of red blood cells has been preferred to the in vivo technique. The in vitro method gives better labeling of red blood cells and a lower quantity of unbound ^{99m}Tc (*30*). Cerebral accumulation of the unbound ^{99m}Tc may occur in our patients with ICA disease and brain infarction and such "trapping" may result in the overestimation of CBV values in infarcted areas. The in vitro technique allows one to minimize this risk.

Compton scatter, attenuation of photons, variable spatial resolution with the distance from the detector and head contour errors are the main factors affecting the images both qualitatively and quantitatively. In spite of recent improvements in SPECT studies, some factors still limit quantitative SPECT. PET has several advantages over SPECT for quantification: improved scatter rejection, better attenuation correction procedures, uniform response of the detection system and higher intrinsic resolution.

To improve quantification in SPECT studies, it is necessary to minimize the major causes of these errors. Correction for Compton scattering and attenuation is more complicated and less accurate for SPECT than for PET. Scatter correction methods have been developed by several authors (*24,31,32*). In our study, we used Jaszczak's method (*24*) with a factor of 0.5. Correction for attenuation was performed in each plane according to the method of Chang (*25*) and assuming a constant linear attenuation coefficient 0.15 cm^{-1}. It is also necessary to determine the margins of the head as accurately as possible. For this purpose, the major axis of ellipses defined for two planes was obtained from the PET data at the same levels.

At low values of CBV, SPECT gave higher values than PET. This overestimation was more pronounced for small ROIs. At high values of CBV, SPECT data were lower than the values obtained by PET, and this underestimation of the value of CBV was also more pronounced for regional ROIs. The same tendency for over- and underestimation was reported previously for CBF measured by SPECT and was explained by the phenomenon of scattered radiation and the partial volume effect

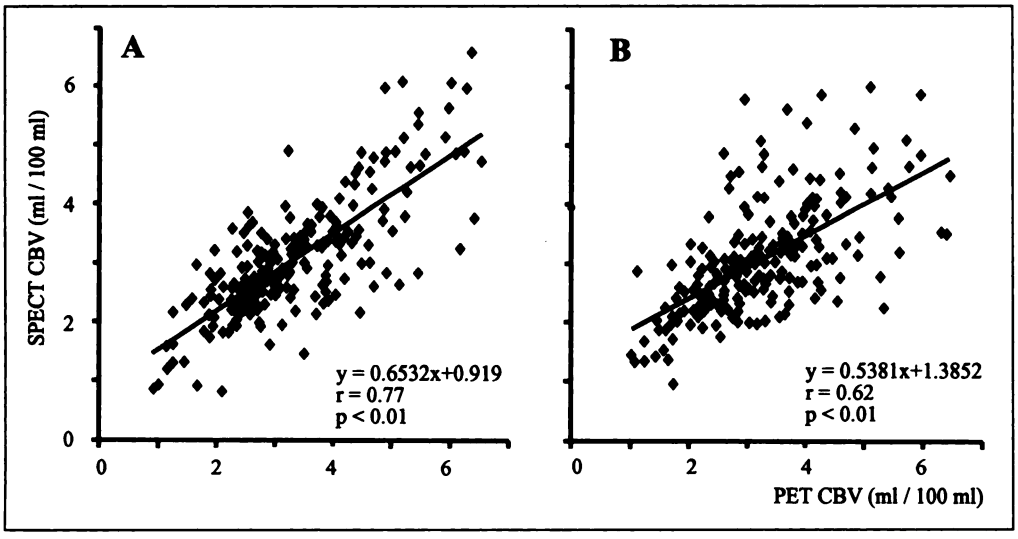

FIGURE 4. Correlation between regional CBV values measured by PET and SPECT in 11 patients with ICA disease for right (A) and left (B) hemispheres.

(*33,34*). In this study, regional CBV quantified using SPECT was 3.09 ± 1.0 ml/100 ml and 3.15 ± 0.93 ml/100 ml for right and left hemispheres, respectively. These values are similar to those previously published by different authors. Hemispheric values for CBV (which included both cortical and subcortical areas) were lower than those measured in regional areas (which included only cortical regions).

In our study, hemispheric CBV values obtained by SPECT and PET were greater for the right hemisphere than for the left hemisphere ($p < 0.01$). However, left hemispheric CBV has been reported to be significantly greater than the right one when studied in right-handed healthy volunteers (*11,28*). It is likely that in patients with brain damage of different origins, such a predominance of left hemisphere is not so evident. Kuhl et al. (*26*) did not find consistent differences in CBV values between right and left hemispheres in head-injured patients. In our series, one of the important factors that may have influenced the value of mean hemispheric CBV was that our patients exhibited different locations and degrees of ICA disease. In some of them, the right ICA was affected, other patients had left ICA stenosis or occlusion and there were also five patients with bilateral ICA diseases.

This factor, as well as the relatively old age of our patients, may partly explain our low mean hemispheric values of CBV as measured by the SPECT and PET studies. Indeed, it has been shown that CBV has a tendency to decrease with age (*23,35*).

CONCLUSION

The results of the study showed a significant correlation between the values of CBV measured by PET and SPECT. Such a finding may be of note to those clinicians who use SPECT technique because PET is not available at many institutions, whereas SPECT is more widely distributed. Lower cost and ease of use (because of the longer half-lives of the radionuclides commonly used in SPECT studies) are advantages that make SPECT more versatile for the quantitative measurement of CBV in routine clinical practice.

As it is possible to obtain quantitative information on CBF, CBV and their ratio, as well as to study the vasodilatory capacity of the cerebrovascular system with acetazolamide, SPECT is therefore an appropriate method for investigating cerebral hemodynamics.

ACKNOWLEDGMENTS

We thank the cyclotron, computer and technical staffs of CYCERON. We are particularly grateful to D. Luet for assistance in preparing the illustrations and to M.-C. Onfroy for the data analysis.

REFERENCES

1. Powers WJ, Raichle ME. Positron emission tomography and its application to the study of cerebrovascular disease in man. *Stroke* 1985;16:361–376.
2. Bullock R, Mendelow AD, Bone I, Patterson J, Macleod WN, Allardice G. Cerebral blood flow and CO_2 responsiveness as an indicator of collateral reserve capacity in patients with carotid arterial disease. *Br J Surg* 1985;72:348–351.
3. Brown MM, Wade JPH, Bishop CCR, Russel RWR. Reactivity of the cerebral circulation in patients with carotid occlusion. *J Neurol Neurosurg Psychiatry* 1986; 49:899–904.
4. Vorstrup S, Brun B, Lassen NA. Evaluation of the cerebral vasodilatory capacity by the acetazolamide test before EC-IC bypass surgery in patients with occlusion of the internal carotid artery. *Stroke* 1986;17:1291–1298.
5. Burt RW, Witt RM, Cikrit DE, Reddy RV. Carotid artery disease: evaluation with acetazolamide-enhanced Tc-99m HMPAO-SPECT. *Radiology* 1992;182:461–466.
6. Gibbs JM, Wise RJS, Leenders KL, Jones T. Evaluation of cerebral blood perfusion reserve in patients with carotid-artery occlusion. *Lancet* 1984;8372:310–314.
7. Powers WJ, Press GA, Grubb RL, Gado M, Raichle ME. The effect of hemodynamically significant carotid artery disease on the hemodynamic status of the cerebral circulation. *Ann Intern Med* 1987;106:27–35.
8. Sette G, Baron JC, Mazoyer B, Levasseur M, Pappata S, Crouzel C. Local brain hemodynamics and oxygen metabolism in cerebrovascular disease: positron emission tomography. *Brain* 1989;112:931–951.
9. Steiger HJ, Aaslid R, Stoos R. Dynamic computed tomographic imaging of regional cerebral blood flow and blood volume. A clinical pilot study. *Stroke* 1993;24:591–597.
10. Derlon JM, Bouvard G, Lechevalier B, et al. Hemodynamic study of internal carotid artery stenosis and occlusions: value of coupled measurements of regional cerebral blood flow and regional cerebral blood volume. In: Meyer JS, ed. *Cerebral vascular disease*, 5th ed. Amsterdam: Elsevier, 1985:170–176.
11. Sakai F, Nakazawa K, Tazaki I, et al. Regional cerebral blood volume and hematocrit measured in normal human volunteers by single photon emission computed tomography. *J Cereb Blood Flow Metab* 1985;5:207–213.
12. Derlon JM, Bouvard G, Lechevalier B, et al. Hemodynamic study of internal carotid artery stenosis and occlusion: value of combined isotopic measurements of regional cerebral blood flow and blood volume. *Ann Vasc Surg* 1986;1:86–97.
13. Toyama H, Takeshita G, Takeuchi A, et al. Cerebral hemodynamics in patients with chronic obstructive carotid disease by rCBF, rCBV and rCBV/rCBF ratio using SPECT. *J Nucl Med* 1990;31:55–60.
14. Sabatini U, Celsis P, Viallard G, Rascol A, Marc-Vergnes JP. Quantitative assessment of cerebral blood volume by single-photon emission computed tomography. *Stroke* 1991;22:324–330.
15. Derlon JM, Bouvard G, Petit MC, et al. Hemodynamic assessment of carotid artery obstructive lesions: comparison of PET and SPECT. In: Schmiedek P, Einhaupl K, Kirsch CM, eds. *Stimulated cerebral blood flow. Experimental findings and clinical significance.* Berlin: Springer-Verlag; 1992:94–110.
16. Inoue Y, Momose T, Machida K, et al. Quantitation of cerebral blood volume by ^{99m}Tc-DTPA-HSA SPECT. *Radiat Med* 1992;10:184–188.
17. Inoue Y, Momose T, Machida K, Honda N, Nishikawa J, Sasaki Y. SPECT measurements of cerebral blood volume before and after acetazolamide in occlusive cerebrovascular diseases. *Radiat Med* 1994;12:245–247.
18. Moore SC. Quantitative capabilities of single-photon emission computed tomography. In: Magistretti PL, ed. *Functional radionuclide imaging of the brain.* New York: Raven Press; 1983:177–192.
19. Frackowiak RSI, Lenzi JG, Jones T, Heather JD. Quantitative measurement of regional cerebral blood flow and oxygen metabolism in man using ^{15}O and positron emission tomography: theory, procedure and normal values. *J Comput Assist Tomogr* 1980;4: 727–736.
20. Fox PT, Perlmutter JS, Raichle ME. A stereotactic method of anatomical localization for positron emission tomography. *J Comput Assist Tomogr* 1985;9:141–153.
21. Talairach J, Tournoux P. *Co-planar stereotaxic atlas of the human brain.* New York: Thieme-Stratton; 1988.
22. Martin WRW, Powers WJ, Raichle ME. Cerebral blood volume measured with inhaled C^{15}O and positron emission tomography. *J Cereb Blood Flow Metab* 1987;7:421–426.
23. Marchal G, Rioux P, Petit-Taboué M-C, et al. Regional cerebral oxygen consumption, blood flow and blood volume in healthy human aging. *Arch Neurol* 1992;49:1013–1020.
24. Jaszczak RJ, Greer KL, Floyd CE, Harris CC, Coleman RE. Improved SPECT quantification using compensation for scattered photons. *J Nucl Med* 1984;25:893–900.
25. Chang LT. A method for attenuation correction in radionuclide computed tomography. *IEEE Trans Nucl Sci* 1978;25:638–643.
26. Kuhl DE, Alavi A, Hoffman EJ, et al. Local cerebral blood volume in head-injured patients: determination by emission computed tomography of ^{99m}Tc-labeled red cells. *J Neurosurg* 1980;52:309–320.
27. Sakai F, Igarashi H, Suzuki S, Tazaki Y. Cerebral blood flow and cerebral hematocrit in patients with cerebral ischemia measured by single-photon emission computed tomography. *Acta Neurol Scand* 1989;127(suppl):9–13.
28. Grubb RL, Raichle ME, Higgins CS, Eichling JO. Measurement of regional cerebral blood volume by emission tomography. *Ann Neurol* 1978;4:322–328.
29. Subramanyam R, Alpert NM, Hoop B, et al. A model for regional cerebral oxygen distribution during continuous inhalation of $^{15}O_2$, C^{15}O and C$^{15}O_2$. *J Nucl Med* 1978;19:48–53.
30. Callahan RJ, Froelich JW, McKusick KA, Leppo J, Strauss HW. A modified method for the in vivo labeling of red blood cells with Tc-99m: concise communication. *J Nucl Med* 1982;23:315–318.
31. Koral KF, Wang X, Rogers WL, Clinthorne NH, Wang X. SPECT Compton-scattering correction by analysis of energy spectra. *J Nucl Med* 1988;29:195–202.
32. Mas J, Ben Younes R, Bidet R. Improvement of quantification in SPECT studies by scatter and attenuation compensation. *Eur J Nucl Med* 1989;15:351–356.
33. Celsis P, Goldman L, Henriksen L, Lassen NA. A method for calculating regional cerebral blood flow from emission computed tomography of inert gas concentrations. *J Comput Assist Tomogr* 1981;5:641–645.
34. Dahl A, Russell D, Nyberg-Hansen R, Rootwelt K, Bakke SJ. Cerebral vasoreactivity in unilateral carotid artery disease. A comparison of blood flow velocity and regional cerebral blood flow measurements. *Stroke* 1994;25:621–626.
35. Leenders KL, Perani D, Lammertsma, et al. Cerebral blood flow, blood volume and oxygen utilization: normal values and effect of age. *Brain* 1990;113:27–47.